2-μm energy-managed soliton fiber laser

Mostafa Mohamed, Aurélien Coillet, Philippe Grelu

2-µm energy-managed soliton fiber laser

MOSTAFA I. MOHAMED[1,2,*], AURÉLIEN COILLET[1], AND PHILIPPE GRELU[1]

[1] Laboratoire Interdisciplinaire Carnot de Bourgogne, UMR CNRS 6303, Université de Bourgogne, 9, Avenue Alain Savary, F-21000 Dijon, France
[2] Department of Physics, Faculty of Science, Alexandria University, Moharram Bek, 21511 Alexandria, Egypt
[*] mostafa.mohamed@u-bourgogne.fr

Compiled October 24, 2024

To generate energetic short pulses from fiber laser oscillators in the 2 µm emission window, we here propose an alternative to the conventional methods of pulse stretching and dispersion management. We build a passively-mode-locked fiber laser from anomalous single-mode fibers and utilize strong dissipative effects to delineate high and low pulse energy sections within the cavity. Whereas the main laser output delivers low-chirp sub-ps pulses with an energy up to 12 nJ, the intracavity pulse is reshaped into a ∼ 0.1-nJ conventional soliton, stabilizing the laser dynamics while enabling a wide tunability in both repetition rate and central emission wavelength.

http://dx.doi.org/10.1364/ao.XX.XXXXXX

The advancement of mode-locked fiber lasers operating at wavelengths around 2 µm has been rapidly progressing, fueled by applications in medicine, environmental sensing, and material processing [1]. Most of these lasers exploit electronic transitions of thulium or/and holmium rare-earth ions within silica fibers to emit in the 1.8 to 2.2 µm range. Passive mode locking is achieved using either saturable absorber compounds such as semiconductors and 1D-2D materials [2], or nonlinear interferences arising from the Kerr nonlinearity, such as within nonlinear fiber loop mirrors or using nonlinear polarization evolution (NPE) [3]. In the 2 µm wavelength window, most silica fibers have anomalous dispersion. Therefore, 2 µm lasers based on standard fibers and operating in the conventional soliton regime typically deliver pulse energies limited to the few hundreds of pJ [4], although recent advances in scaling down the fiber cavity length achieved nJ pulse level at high repetition rate [5].

To go beyond the previous pulse energy limitation, several methods have been implemented to reach output pulse energies in the 1-100 nJ range from single fiber laser oscillators [6]. A popular approach relies on generating highly-chirped pulses, therefore reducing the nonlinearity impairments for a given pulse energy. Successful demonstrations include dispersion management [7], self-similar dynamics [8] as well as Mamyshev oscillators [9, 10]. These solutions require normal dispersion media, which are difficult to obtain and combine with standard silica fibers at 2 µm. Dispersion-managed cavities have thus been implemented through innovative yet complicated solutions: specialty low dispersion fluoride fibers [11], silica microfibers [12], small-core fibers [8], W-index profile gain fibers [13] or free-space grating compressors [14]. An additional drawback of dispersion-engineered mode-locked fiber lasers is that the output pulse is highly chirped, thus requiring a pulse compression stage at the laser output. The other main approach to upscale the pulse energy consists in using large mode area fibers, which also requires very technical fiber fabrication processes and delicate fiber handling [15].

In the present work, we propose to exploit the potential of dissipative effects to upscale the output pulse energy by more than an order of magnitude in an all-anomalous dispersion thulium-doped mode-locked fiber laser. By applying strong intracavity dissipative effects, we delineate high and low pulse energy propagation sections, which we call energy-management [16]. In the low energy section, conventional soliton propagation takes place in a passive fiber whose length can be therefore be set quite arbitrarily. The high energy section is defined by a limited stretch of a high-gain fiber amplifier, also anomalously dispersive. Energy

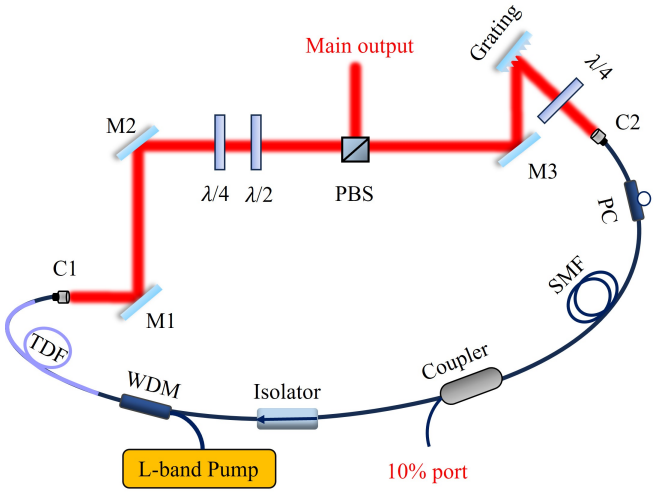

Fig. 1. 2-µm energy-managed soliton fiber laser setup. SMF: single mode fiber; WDM: wavelength-division multiplexer; TDF: Thulium-doped fiber; C1, C2: fiber collimators ; PBS: polarization beam splitter; M1, M2 and M3: mirrors; PC: polarizer controler. All fibers have anomalous dispersion.

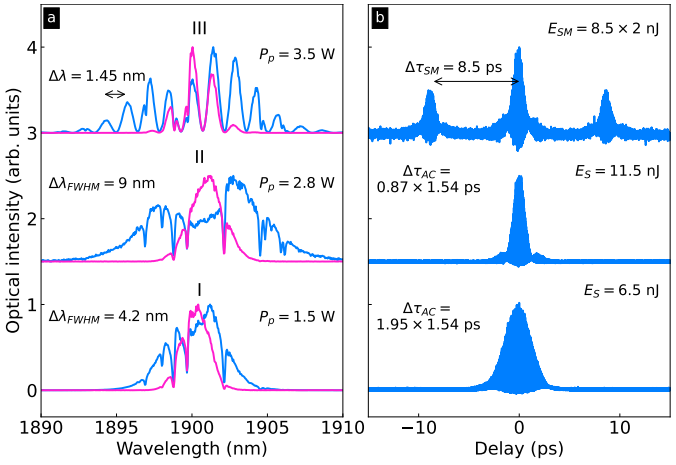

Fig. 2. Mode-locked regimes at 27.6 MHz repetition rate. (a) and (b) showcase the normalized output pulse spectra and interferometric auto-correlation traces. Rows I and II depict single-pulse regimes at pump powers $P_p = 1.5$ W and 2.8 W, respectively. Row III characterizes a soliton molecule at $P_p = 3.5$ W. The main laser output (from PBS) is shown in blue curves, while the 10% port is in pink. E_S is the energy of a single pulse, while E_{SM} is the energy of the soliton molecule.

management implies dumping most of the pulse energy – typically above 90% – through a main output port before applying spectral filtering. The main role of spectral filtering is to reshape the pulse and start the conventional soliton propagation in the passive fiber, noting also that an adjustable filter allows controlling the laser central wavelength. Indeed, spectral tunability is of particular interest for thulium-holmium fiber lasers, which feature a potential broadband gain spanning from 1.8 to 2.2 µm [5, 17, 18]. The proposed energy-managed laser architecture is self-starting and yields a robust mode locked operation. The combination of two widely different pulse dynamics connected by spectral filtering constitutes a common point between the energy-managed laser recently demonstrated in Ref. [16] at 1.5 µm emission wavelength and the soliton-similariton laser proposed in 2010 [19]. Nevertheless, these two laser architectures feature major differences, as the energy-management scheme does not involve any dispersion management and yields energetic pulses with a limited frequency chirping. We here show the benefits of the energy-managed laser architecture in the case of a thulium fiber laser where, as a proof of principle, we restrict to the usage of standard optical fibers. We demonstrate the generation of 10 nJ pulses at an adjustable repetition rate from 12 to 33 MHz and a central wavelength spanning from 1850 to 1960 nm.

Figure 1 depicts the experimental 2-µm energy-managed soliton fiber laser. The gain medium is a 3-meter-long thulium-doped fiber with anomalous dispersion (TDF), which has a mode filed diameter (MFD) of 10.4 µm at the wavelength of 1.9 µm, pumped at 1567 nm by a continuous wave erbium fiber laser coupled through a wavelength-division multiplexer and delivering up to 5 W. After the gain medium, a free-space section with wave plates and a polarizing beam splitter (PBS) allow for a precise control of the NPE-based saturable absorber transfer function. The PBS rejection port serves as the primary laser output [20, 21], which is here set to extract over 90% of the intracavity power. Spectral filtering and central wavelength tuning are also achieved in the free-space section through the combination of a grating (600 lines per millimeter) and a collimator that couples the light back into a single-mode fiber (SMF-28e, MFD = 10.9 µm at 1.9 µm wavelength). The rest of the cavity consists of a 10% coupler for additional monitoring and a polarization-insensitive isolator ensuring unidirectional lasing. Both laser outputs are analyzed using a 12 GHz photodiode connected to an 8 GHz oscilloscope (OSC), a 250-ps delay interferometric autocorrelator for time-domain analysis, and a time-averaged, grating-based optical spectrum analyzer (OSA) operating in the 1.2–2.4 µm range.

At a pumping power of 1.5 W, after adjusting the wave plates orientations, self-starting mode locking is obtained at the fundamental repetition rate of the cavity, first set at 27.6 MHz. The time-domain and frequency-domain characterization of the generated pulses are shown in the lower row (I) of Fig. 2. Besides water absorption lines, the pulse spectrum has a smooth bell shape devoid of the Gordon-Kelly sidebands that plague most of the spectra of anomalous fiber lasers [22, 23], especially at 2 µm wavelength owing to the large fiber dispersion. The main output (PBS) yields 180 mW of average power, a pulse duration of 1.95 ps. The pulse energy is 6.5 nJ, about two orders of magnitude greater than the conventional soliton energy that would be supported by the standard anomalous optical fiber, assuming the same pulse duration. As a matter of fact, the secondary (10% coupler) output measures an average power of 0.215 mW, which corresponds to 7.8-pJ output pulses and therefore to 78-pJ pulses propagating in the intracavity SMF. The high pulse energy obtained from the main output, combined with a lack of radiation sidebands, results from the highly dissipative cavity design, which incorporates large nonlinear losses, high gain, and significant spectral filtering [16].

For the laser pulse, increasing the pumping power to 2.8 W entails a higher peak power, thus a larger accumulated nonlinear phase broadening the spectrum, see the blue curve in Fig. 2a, row II. Then, soliton pulse shaping within the anomalous gain fiber induces a significant pulse compression, see Fig. 2b row II. The average main output power is then 317 mW, corresponding to a pulse energy of 11.5 nJ and a peak power of 13.2 kW for a measured pulse duration of 0.87 ps. Such remarkable result for the use of standard anomalous fibers composing the laser cavity can be interpreted as arising from the gradual higher-order soliton formation and compression along the gain fiber, with an estimated output soliton order of N $\sim$ 5, calculated using the Fourier-transform limited pulse duration of 420 fs [16, 24]. Any further increase in the pump power – all other laser parameters being fixed – leads to soliton fission and the formation of soliton molecules. The upper row (III) of Fig. 2 shows the characterization of a stable higher-order soliton molecule (HOSM) consisting of two bound pulses separated by 8.5 ps, having an energy of 17 nJ, average power of 469 mW at a pump power of 3.5 W.

To deepen our understanding of the intracavity dynamics, we conducted numerical simulations of the energy-managed fiber laser cavity using a lumped model based on the generalized Schrödinger equation as in Ref. [25], with adapted parameters corresponding to the present cavity. By adjusting the saturation power of the saturable absorber transfer function and the amplifier saturation energy, we were able to reproduce the pulse regime shown in Fig 2 row II. Starting from random noise, stationary mode locking is numerically obtained after a few tens of cavity roundtrips. Then, the intracavity pulse evolution is shown in Fig. 3. It confirms that the amplification section (TDF) provides a large gain of around 20 dB to the incoming low-energy,

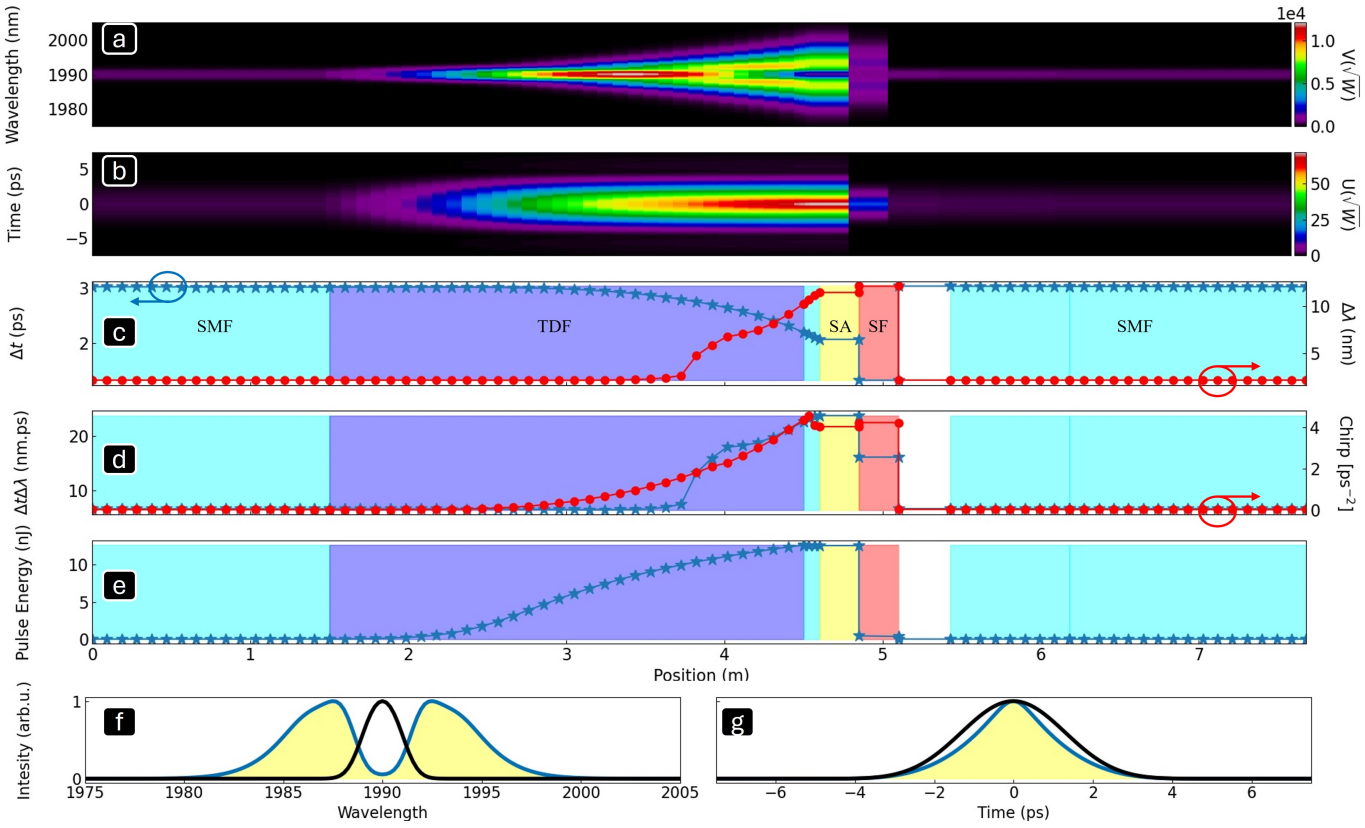

Fig. 3. Numerical simulation of the pulse propagation along one cavity roundtrip in the stationary regime. Colormaps of the time-domain (a) and spectral (b) fields evolution. (c) Evolution of the pulse width (FWHM, blue curve) and the spectral width (FWHM, red curve). SA: saturable absorber, SF: spectral filter. (d) Evolution of the time-bandwidth product (FWHM, blue curve) and the frequency chirp (red curve). (e) Evolution of the pulse energy. (f) Snapshots of the spectrum and (g) time-domain profile from the main (blue curves) and 10% (black curves) output ports.

narrow-spectrum pulse. Halfway through the gain fiber, as the peak power of the amplified pulse reaches 10-kW level, the Kerr nonlinearity starts affecting the pulse propagation: self-phase modulation (SPM) broadens and splits the spectrum in two lobes, whereas nonlinear pulse compression occurs in the time domain. The calculated accumulated nonlinear phase (B-integral) yields a value close to 2π along the TDF, which is consistent with the formation of these pronounced spectral lobes. Right after the amplification stage, the saturable absorber extracts around 90% of the energy from the cavity, corresponding to the PBS output of the experimental setup. The yellow-filled blue curves of Fig. 3 (f) and (g) show, respectively, the snapshots spectrum and time-domain intensity profile at this stage, in good agreement with the experimental results displayed, in Fig. 2 row II. The subsequent operation of spectral filtering leads to the formation of a smooth, bell-shaped pulse that propagates without deformation within the single-mode fiber as a conventional soliton.

The graphs of Fig. 3 (c), (d) and (e) provide additional information regarding the characteristics of the pulse at different positions within the cavity, and further support the previous discussion: in addition to bringing up the energy to 13 nJ, the amplification section also broadens the spectrum from 2 to 12 nm, compresses the pulse down from 3 to 2 ps, owing to the SPM-induced positive chirp. After the amplification stage, the pulse is not Fourier-transform limited, but both the losses induced by the saturable absorber and the spectral filtering effectively remove most of the chirp, allowing for a soliton-like propagation upon re-coupling into a standard SMF fiber.

Such distortion-less propagation provides an additional flexibility to the laser cavity: the length of that SMF can be changed arbitrarily, and thus the repetition rate of the laser too. The experimental results shown in Fig. 4 (a) and (b) validate this useful feature: the repetition rate can be decreased down to 12 MHz by adding up to 10 meters of SMF, while maintaining a single-pulse mode-locked regime with nearly identical pulse features. The generated pulses maintain their shape with a pulse energy of approximately 6 nJ at the main output (Fig. 4 (a)), throughout the full repetition rate range. Maintaining the pulse energy while lowering the repetition frequency results in a reduction of the required pump power, as shown in Fig. 4 (b). Further addition of SMF length could in principle bring down the repetition rate to below the MHz range, but other physical effects can disrupt the stability of the mode-locked operation, such as gain relaxation dynamics or the impact of fiber losses.

In addition to the tunability of the repetition rate, the diffraction grating enables further flexibility by permitting the adjustment of the central wavelength of the laser emission. This aspect is particularly significant for Tm-doped fiber lasers, whose broad gain bandwidths allow for an extended tunability. The experimental spectra shown in Fig. 4(c) confirm this possibility: starting with a single-pulse mode-locked state at 1900 nm, we are able to tune its central wavelength over a 100-nm window. It

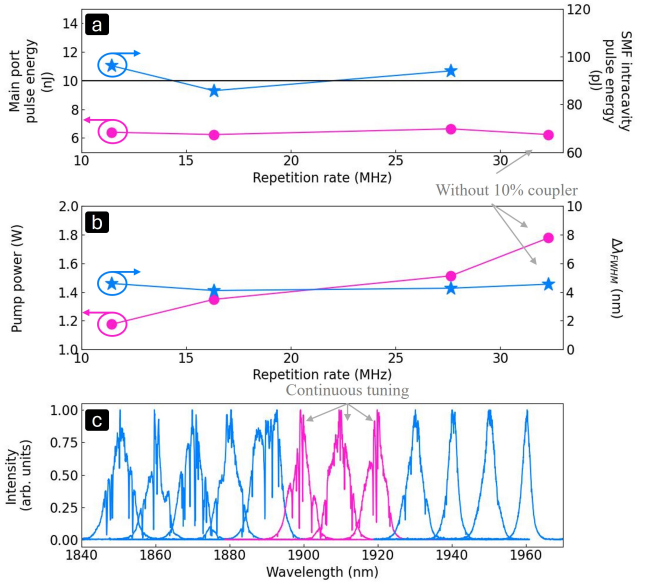

Fig. 4. Experimental laser flexibility over the repetition rate and central wavelength. Single pulse features are obtained by changing the SMF fiber length while fixing the pulse energy close to 6 nJ. (a) The main laser output pulse energy (in pink) and the intracavity pulse energy along the SMF part (in blue) compared with the conventional (N=1) soliton energy (90 pJ for a 2.65-ps FWHM pulse). (b) The corresponding pump power (in pink) and pulse bandwidth of the main laser output port (in blue). (c) Wavelength-tunable mode-locked spectra recorded every 10 nm. Pink curves for continuous tuning through the sole grating orientation.

should be noted that central wavelength tuning within 20 nm of the initial mode-locked state can be achieved continuously, by solely changing the grating orientation, without adjustment of any other cavity parameters. For larger wavelength excursions, the coupling collimator C2 and the quarter-wave plate need to be slightly realigned. Following this procedure, single-pulse mode-locked regimes with similar spectra are obtained over the 100-nm window.

To summarize and conclude, we reported a passively mode-locked fiber laser emitting up to 12 nJ pulses with a central wavelength tunable from 1.85 to 1.96 µm. As a proof of concept, the proposed 2-µm laser architecture uses standard commonly available anomalous-dispersion fibers, in contrast to dispersion-managed cavities requiring normal dispersion elements that are difficult to utilize in this spectral band. Multi-pulse and unstable regimes are avoided by extracting most of the intracavity energy right after the gain fiber, preventing additional detrimental nonlinear propagation effects. The energy-managed laser dynamics, which is an intimate combination of (overall) dissipative soliton and (locally) conventional soliton dynamics [26], finds its best applications within fiber lasers operating at wavelengths above 1.5 µm. A path for further increasing the output pulse energy would therefore be to use a more highly-doped fiber, such that pulse amplification would occur on a shorter fiber length scale, with lower accumulated nonlinear effects. After the main output coupler, a spectral filter removes Kerr-induced spectral broadening, effectively resetting the pulse close to a conventional soliton for the remainder of the cavity propagation in passive anomalous fiber, whose arbitrary length is used to alter the fundamental laser repetition rate in a broad range. We also show that the broadband gain of thulium amplifiers can be further exploited by allowing a wide tunability of the central wavelength through the tuning of the intracavity spectral filter. We anticipate that fiber lasers based on co-doped thulium-holmium gain fibers could expand this tunability further, potentially reaching 2.1 µm. The spectral filtering could in future works also be leveraged to tune the pulse duration. These improvements combined together would make for an extremely versatile, compact and low-cost, high-energy pulsed fiber laser oscillator.

Funding. The authors acknowledge support from the CEFIPRA project "TUFL".

Disclosures. The authors declare no conflicts of interest.

Data availability. Data underlying the results presented in this paper are not publicly available at this time but may be obtained from the authors upon reasonable request.

REFERENCES

1. C. W. Rudy, M. J. F. Digonnet, and R. L. Byer, Opt. Fib. Technol. **20**, 642 (2014).
2. L. C. Silva and M. E. Segatto, Opt. Fiber Technol. **78**, 103310 (2023).
3. S. Hamdi, A. Coillet, and P. Grelu, Opt. Lett. **43**, 4965 (2018).
4. L. E. Nelson, E. P. Ippen, and H. A. Haus, Appl. Phys. Lett. **67**, 19 (1995).
5. K. Wei, H. Zhang, K. Yang, *et al.*, Opt. Lett. **47**, 1545 (2022).
6. J. Ma, Z. Qin, G. Xie, *et al.*, Appl. Phys. Rev. **6**, 021317 (2019).
7. A. Wienke, F. Haxsen, D. Wandt, *et al.*, Opt. Lett. **37**, 2466 (2012).
8. Y. Tang, A. Chong, and F. W. Wise, Opt. Lett. **40**, 2361 (2015).
9. P. Repgen, B. Schuhbauer, M. Hinkelmann, *et al.*, Opt. Express **28**, 13837 (2020).
10. B. Schuhbauer, V. Adolfs, F. Haxsen, *et al.*, Opt. Lett. **47**, 5610 (2022).
11. Y. Nomura and T. Fuji, Opt. Express **22**, 12461 (2014).
12. Y. Li, L. Wang, Y. Kang, *et al.*, Opt. Lett. **43**, 6105 (2018).
13. Y. Chen, S. Yoo, S. Chen, *et al.*, IEEE Photonics J. **11**, 1 (2019).
14. F. Haxsen, D. Wandt, U. Morgner, *et al.*, Opt. Express **18**, 18981 (2010).
15. Z. Zhu, H. Zhang, M. Wang, *et al.*, IEEE Photonics Technol. Lett. **32**, 117 (2020).
16. M. Mohamed, A. Coillet, and P. Grelu, Nat. Commun. **15**, 8875 (2024).
17. X. Liu, J. K. Sahu, and R. Gumenyuk, Opt. Lett. **48**, 612 (2023).
18. A. Grande, D. Darwich, V. Freysz, *et al.*, Opt. Lett. **48**, 5237 (2023).
19. B. Oktem, C. Ülgüdür, and F. Ilday, Nat. Photonics **4**, 307 (201O).
20. K. Tamura, C. R. Doerr, L. E. Nelson, *et al.*, Opt. Lett. **19**, 46 (1994).
21. B. Ortaç, A. Hideur, M. Brunel, *et al.*, Appl. Phys. B **77**, 589 (2003).
22. S. Kelly, Electron. Lett. **28**, 806 (1992).
23. J. P. Gordon, J. Opt. Soc. Am. B **9**, 91 (1992).
24. C. Gao, Z. Wang, H. Luo, and L. Zhan, J. Light. Technol. **35**, 2988 (2017).
25. Z. Wang, A. Coillet, S. Hamdi, *et al.*, Laser Photonics Rev. **17**, 2200298 (2023).
26. P. Grelu, Opt. Commun. **552**, 130035 (2024).

FULL REFERENCES

1. C. W. Rudy, M. J. F. Digonnet, and R. L. Byer, "Advances in 2-micron tm-doped mode-locked fiber lasers," Opt. Fib. Technol. **20**, 642–649 (2014).
2. L. C. Silva and M. E. Segatto, "Recent advances in thulium-doped fiber lasers based on saturable absorber materials at 2000 nm," Opt. Fiber Technol. **78**, 103310 (2023).
3. S. Hamdi, A. Coillet, and P. Grelu, "Real-time characterization of optical soliton molecule dynamics in an ultrafast thulium fiber laser," Opt. Lett. **43**, 4965–4968 (2018).
4. L. E. Nelson, E. P. Ippen, and H. A. Haus, "Broadly tunable sub-500 fs pulses from an additive-pulse mode-locked thulium-doped fiber ring laser," Appl. Phys. Lett. **67**, 19–21 (1995).
5. K. Wei, H. Zhang, K. Yang, *et al.*, "Tunable thulium-doped mode-locked fiber laser with watt-level average power," Opt. Lett. **47**, 1545–1548 (2022).
6. J. Ma, Z. Qin, G. Xie, *et al.*, "Review of mid-infrared mode-locked laser sources in the 2.0 µm–3.5 µm spectral region," Appl. Phys. Rev. **6**, 021317 (2019).
7. A. Wienke, F. Haxsen, D. Wandt, *et al.*, "Ultrafast, stretched-pulse thulium-doped fiber laser with a fiber-based dispersion management," Opt. Lett. **37**, 2466–2468 (2012).
8. Y. Tang, A. Chong, and F. W. Wise, "Generation of 8 nj pulses from a normal-dispersion thulium fiber laser," Opt. Lett. **40**, 2361 (2015).
9. P. Repgen, B. Schuhbauer, M. Hinkelmann, *et al.*, "Mode-locked pulses from a thulium-doped fiber mamyshev oscillator," Opt. Express **28**, 13837–13844 (2020).
10. B. Schuhbauer, V. Adolfs, F. Haxsen, *et al.*, "Generation of 15 nj pulse energy by a sub-150 fs thulium-doped fiber mamyshev oscillator," Opt. Lett. **47**, 5610–5613 (2022).
11. Y. Nomura and T. Fuji, "Sub-50-fs pulse generation from thulium-doped zblan fiber laser oscillator," Opt. Express **22**, 12461 (2014).
12. Y. Li, L. Wang, Y. Kang, *et al.*, "Microfiber-enabled dissipative soliton fiber laser at 2 µm," Opt. Lett. **43**, 6105–6108 (2018).
13. Y. Chen, S. Yoo, S. Chen, *et al.*, "High energy ultrafast laser at 2 µm using dispersion engineered thulium-doped fiber," IEEE Photonics J. **11**, 1–12 (2019).
14. F. Haxsen, D. Wandt, U. Morgner, *et al.*, "Pulse characteristics of a passively mode-locked thulium fiber laser with positive and negative cavity dispersion," Opt. Express **18**, 18981 (2010).
15. Z. Zhu, H. Zhang, M. Wang, *et al.*, "Soliton mode-locked large-mode-area tm-doped fiber oscillator," IEEE Photonics Technol. Lett. **32**, 117–120 (2020).
16. M. Mohamed, A. Coillet, and P. Grelu, "Energy-managed soliton fiber laser," Nat. Commun. **15**, 8875 (2024).
17. X. Liu, J. K. Sahu, and R. Gumenyuk, "Tunable dissipative soliton tm-doped fiber laser operating from 1700 nm to 1900 nm," Opt. Lett. **48**, 612–615 (2023).
18. A. Grande, D. Darwich, V. Freysz, *et al.*, "Sub-100 fs all-fiber polarization maintaining widely tunable laser at 2 µm," Opt. Lett. **48**, 5237–5240 (2023).
19. B. Oktem, C. Ülgüdür, and F. Ilday, "Soliton-similariton fiber laser," Nat. Photonics **4**, 307–311 (201O).
20. K. Tamura, C. R. Doerr, L. E. Nelson, *et al.*, "Technique for obtaining high-energy ultrashort pulses from an additive-pulse mode-locked erbium-doped fiber ring laser," Opt. Lett. **19**, 46–48 (1994).
21. B. Ortaç, A. Hideur, M. Brunel, *et al.*, "Characterization of an ytterbium-doped double-clad fiber laser passively mode-locked by nonlinear polarization rotation," Appl. Phys. B **77**, 589–594 (2003).
22. S. Kelly, "Characteristic sideband instability of periodically amplified average soliton," Electron. Lett. **28**, 806 (1992).
23. J. P. Gordon, "Dispersive perturbations of solitons of the nonlinear schrödinger equation," J. Opt. Soc. Am. B **9**, 91–97 (1992).
24. C. Gao, Z. Wang, H. Luo, and L. Zhan, "High energy all-fiber tm-doped femtosecond soliton laser mode-locked by nonlinear polarization rotation," J. Light. Technol. **35**, 2988–2993 (2017).
25. Z. Wang, A. Coillet, S. Hamdi, *et al.*, "Spectral pulsations of dissipative solitons in ultrafast fiber lasers: Period doubling and beyond," Laser Photonics Rev. **17**, 2200298 (2023).
26. P. Grelu, "Solitary waves in ultrafast fiber lasers: From solitons to dissipative solitons," Opt. Commun. **552**, 130035 (2024).